Computation of the Mutual Inductance between Rotor and Stator of Synchronous Claw-Pole Alternators regarding Claw Chamfers

St. Schulte, K. Hameyer
Institute of Electrical Machines
RWTH Aachen University
Schinkelstr. 4 52056 Aachen Germany
stephan.schulte@iem.rwth-aachen.de

Abstract
This paper describes two approaches for the computation of the mutual inductance between rotor and stator of synchronous claw-pole alternators with respect to the distinctive claw-shape. There is no direct access to measure the mutual inductance which requires an indirect determination. Due to the complex design of the rotor, the computational approaches are non-trivial.
If prototypes are available, the mutual inductance can be computed on the basis of the synchronous-generated voltage measured at no-load operation. Appliance of a Fourier analysis on the determined characteristic of the mutual inductance, contained harmonics are provided, to allow for analytic composition.
At early design stages the mutual inductance need to be determined analytically due to the lack of prototypes. A Matlab tool is utilized to compute the mutual inductance dependent on chamfer angle and chamfer width.

I. INTRODUCTION

Automotive applications are mostly designed to low costs. Efforts to reduce noise, increase efficiency, and expand life time call for optimized machine designs. Nowadays the utilization of computational analysis allows for the substitution of expensive prototype construction at early design stages. Authentic simulations of the real machine behavior require advanced component modeling. The description of two options for the determination of the mutual inductance between rotor and stator of synchronous claw-pole alternators with respect to the distinctive claw-shape is subject of this paper.
Claw-pole alternators belong to the category of salient-pole synchronous machines. This type of machines is characterized by position dependent mutual inductances between the rotor and the stator phases.
The electromagnetic machine behavior and its interaction with rectifier bridge, load and vehicle-power supply-system is usually analyzed as spatio-temporal description. Therefore, the distinctive 3D shape of the rotor needs to be projected into a 2D plane – variable vs. time (the latter is equivalent to position).

II. DETERMINATION OF THE MUTUAL INDUCTANCE FOR OPTIMIZATION PURPOSES

The subsequent computation approach requires the availability of real machines for measurement purposes. The mutual inductance cannot be measured directly so that its determination is processed indirectly. Measuring the induced voltage U_P (synchronous generated voltage) is found most reasonable since U_P is a 2D (quantity vs. time/position) value and furthermore easily accessible at the terminals at no-load operation [1].

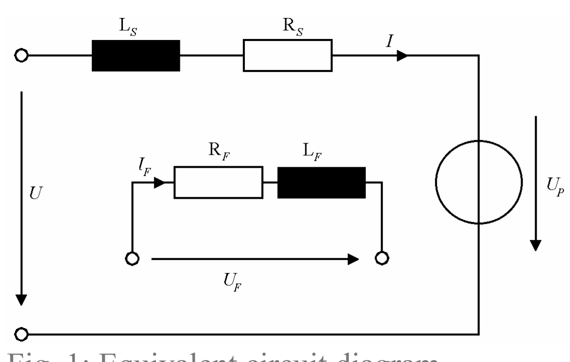

Fig. 1: Equivalent circuit diagram.

The real machine is driven at constant speed and excitation with open terminals (I=0) – see Fig. 1 for the applicable equivalent circuit diagram (indices S=stator, F=field, rotor) [1].

$$U_P = \omega \cdot L_{FS} \cdot I_F \quad (1)$$

$$U_P = \frac{dL_{FS}}{dt} \cdot I_F \quad (2)$$

$$L_{FS} = \int_t \frac{U_P}{I_F} dt \quad (3)$$

U_P states the basis for the determination of the mutual inductance L_{FS} between rotor and stator according to equations (1)-(3).
A general expression for the mutual inductance L_{FS} is given in (4) for stator phase U, only considering the fundamental for clarity reasons, a typical characteristic of L_{FS} is illustrated in Fig. 2 for a selected period.

$$L_{FS\_U} = \mathrm{L}_d \cdot \cos(\gamma), \quad \text{with } \gamma = \gamma_0 + \int \omega \; dt \quad (4)$$

Application of a Matlab [2] implemented Fourier analysis routine on the resulting plot of L_{FS} results in the contained harmonics (Fig. 3).

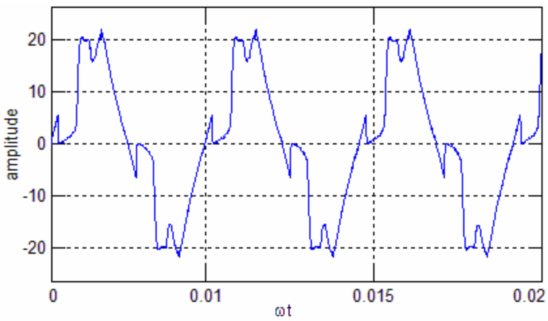

Fig. 2: Plot of L_{FS} vs. ωt.

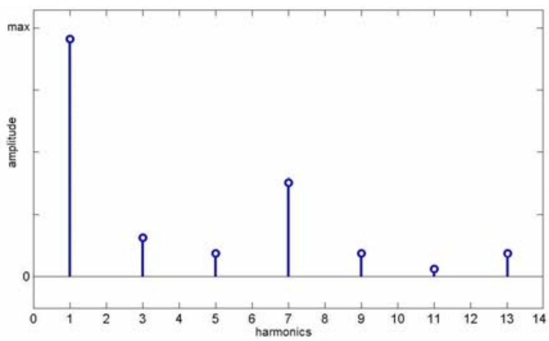

Fig. 3: Harmonics content.

Data thus obtained is to be synthesized to form an equation to describe the spatio-temporal mutual inductance, utilized in circuit-based simulations.
Coverage of design-specific originalities such as the particular claw shape (Fig. 4), influence of the claw chamfer and, therefore, the pole-pitch factor, automatically to come along with measurement of the synchronous generated voltage, is one of the benefits of this scheme.


Fig. 4: Rotor with claws (iron part).

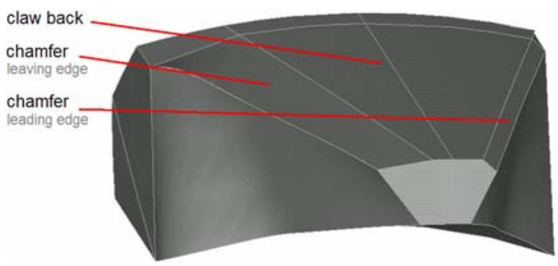

Fig. 5: Cut out of a single claw finger

The ability of authentically describing the mutual inductance of a real machine allows for setting up a claw-pole alternator-model for circuit based simulations. These simulations are used for investigation and optimization purposes.

III. DETERMINATION OF THE MUTUAL INDUCTANCE FOR GENERAL DESIGN PURPOSES

At the earliest stage of the design process with no existing prototypes, the scheme described in section 2 is unfortunately not applicable. That requires an analytic determination of the mutual inductance between rotor and stator [2], [3], based on geometric and material specific parameters. As to be shown in the full paper, the constant factor L_d from (4) computes to

$$L_d = \frac{\mu \cdot w_S \cdot l_{ax} \cdot d \cdot w_F \cdot k}{2 \cdot p \cdot \delta_0''} \qquad (5)$$

with μ: permeability, w_S: No. stator windings, l_{ax}: axial length, d: diameter of rotor, w_F: No. of rotor windings, k: gathering various constants, p: pole pairs, δ_0'': effective air-gap width.

Equation (5) accords to a ratio of effective air-gap surface per effective air-gap width

$$L_d = c \cdot \frac{l_{ax} \cdot d}{\delta_0''}. \qquad (6)$$

$$c = \frac{\mu \cdot w_S \cdot w_F \cdot k}{2 \cdot p} \qquad (7)$$

For unchamfered claws, the surface of the claw back is planar, hence a homogeneous air-gap width is assumed above the claw, keeping the model of the mutual inductance easy.

A cross section of both, unchamfered and chamfered rotor is depicted in Fig. 6 (a, b).

Fig. 6: Cross section of claw and air gap

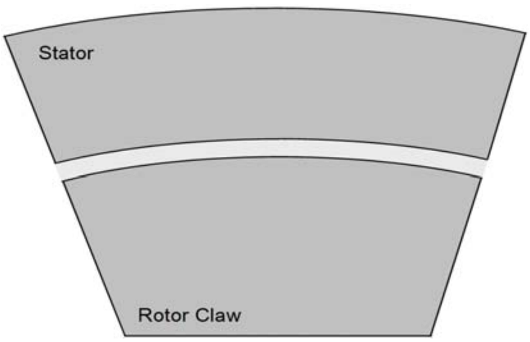

Fig. 6a: Unchamfered claw.

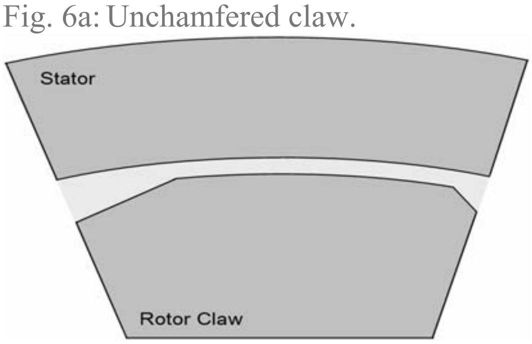

Fig. 6b: Chamfered claw.

This simplification is used to the disadvantage of mutual-inductance peak-value errors up to 10%, leading to proportional current errors compared to measured values taken as a reference from earlier machines. The consideration of the claw chamfer complicates the computation of the mutual inductance due to locally increasing air-gap widths.

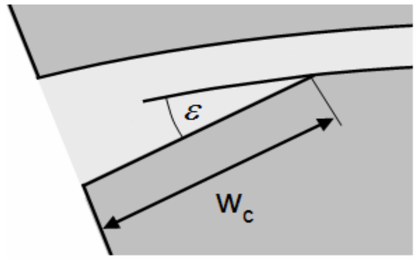

Fig. 7: Cut out of the chamfer cross section.

Figure 7 depicts a cut out of the chamfer based on the rotor-stator arrangement due to Figure 6b. Solely the chamfer on the leaving edge of the claw is shown - analogous chamfer angle and width apply for the leading edge.

A Matlab tool is implemented to compute the constant factor of the mutual inductance between rotor and stator dependent on the chamfer angle ε and the chamfer width w_c analytically. Figure 8 shows L_d vs. reasonable ranges of ε and w_c. This analytical Matlab tool allows for a variation of the claw chamfer dimensions, directly affecting the factor L_d and, therefore, the stator current. A reasonable angle ε and chamfer width w_c need to be chosen to have Matlab determine the accordant L_d. This L_d is available for circuit based simulations to determine the corresponding stator current due to (4).

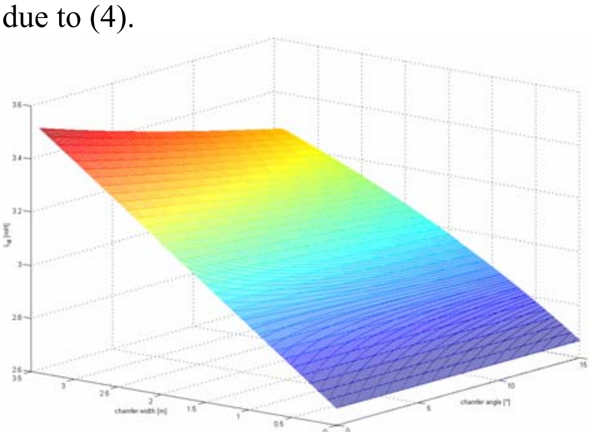
Fig. 7: Matlab plot of mutual inductance L_d vs. chamfer angle ε and width w_c.

IV. RESULTS

Mutual inductance L_d values resulting from analytical computation match Finite-Elements (FE) simulation-results very well. This applies for single operational states of the claw-pole alternator, characterized by excitation and rotational speed, which affect the applicable permeability μ. Under laying a look-up table containing the speed/excitation dependency of the permeability μ allows for universal computation of any operational point. The accordant look-up table needs to be determined previously, e.g. using FE models. Appliance of the under laid permeability matrix will be presented in the full paper.

V. CONCLUSION

This paper describes two options for the determination of the mutual inductance between rotor and stator of synchronous claw-pole alternators. If prototypes are available, the mutual inductance can be computed on the basis of the synchronous-generated voltage measured at no-load operation. Appliance of a Fourier analysis on the determined characteristic of the mutual inductance, contained harmonics are provided, to allow for analytic evaluation. Description of the obtained mutual inductance can be utilized for implementation of circuit-based simulations.

At early design stages the mutual inductance need to be determined analytically due to the lack of prototypes. A Matlab tool is implemented to compute the mutual inductance dependent on chamfer angle and chamfer width. These parameters can be either chosen as single scalar values or as vectors covering angle and width ranges.

Results from the analytical determination of the mutual inductance with utilization in circuit-based simulations lead to currents matching measured currents very well.

However, in order to improve the simulation model in terms of the mutual inductance, a description of leakage and saturation is to be regarded yet.

REFERENCES

[1] G. Henneberger, Elektrische Motoren-ausrüstung für Kraftfahrzeuge (Electrical Machine Equipment for Vehicle Power Supply Systems), Vieweg, 1990

[2] Matlab, The MathWorks, Inc., homepage: www.matlab.com